

Structural performance of lightweight fibre-reinforced oil palm shell concrete subjected to impact loadings under varying boundary conditions

Idris Ahmed Ja'e^{a,b,*}, Zakaria Che Muda^{c,**}, Agusril Syamsir^a, Chiemela Victor Amaechi^{a,**}, Hamad Almujibah^d, Ali.E.A. Elshekh^d, Maaz Osman Bashir^d, Abdulrazak H. Almaliki^d

^a Institute of Energy Infrastructure, Universiti Tenaga Nasional, Putrajaya Campus, Jalan IKRAM-UNITEN, Kajang, Selangor 43000, Malaysia

^b Department of Civil Engineering, Ahmadu Bello University, Zaria 810107, Nigeria

^c Faculty of Engineering and Quantity Surveying, INTI-International University, Persiaran Perdana BBN Putra Nilai, Nilai 71800, Malaysia

^d Department of Civil Engineering, College of Engineering, Taif University, P.O. Box 11099, Taif City 21974, Saudi Arabia

ARTICLE INFO

Keywords:

Waste recycling
Oil palm shell aggregate
Energy
Impact behaviour
Polypropylene fibres
Polypropylene mesh
Boundary condition

ABSTRACT

Lightweight concrete produced from recycled agricultural waste, has been used for decades as an eco-friendly product. This innovative approach aims to mitigate environmental pollution and promote sustainable practices in managing industrial waste. Despite these benefits, there is a limited study on the structural behaviour of lightweight oil palm shells (OPS) concrete with varying boundary conditions. This study conducted a series of low-velocity impact loading tests to investigate the structural performance of lightweight fibre-reinforced OPS concrete slabs, in which the natural aggregate is completely replaced with OPS. The slab specimens sized 300 mm x 300 mm x 40 mm were used. The control sample contained polypropylene fibre (PPF) mesh at mid-layer, in addition, other specimens contain 1 %, 2 % and 3 % PPF content. For each PPF content in the experimental specimens, the boundary conditions were varied from 2, 3 and 4 including the control case. The recorded experimental results for impact and crack behaviour under service and ultimate loading were analysed using response surface analysis. Regression models were developed to predict responses for specimens with up to 8 boundary conditions and 5 % PPF. The results demonstrated the effectiveness of OPS as a coarse aggregate in lightweight concrete, showing substantial enhancements in impact energy absorption (up to 20 times at ultimate loading), crack resistance (up to 29 times at ultimate loading) and reduction in crack propagation with increased PPF and varying boundary conditions. Furthermore, the incorporation of PPF also enhanced the OPS concrete's resistance to cracking relative to its compressive strength. However, these only had a minimal influence on controlling crack length and width, and did not result in reasonable improvement of the residual strength. These findings highlight the

* Corresponding author at: Institute of Energy Infrastructure, Universiti Tenaga Nasional, Putrajaya Campus, Jalan IKRAM-UNITEN, Kajang, Selangor 43000, Malaysia.

** Corresponding authors.

E-mail addresses: idris.ahmad@uniten.edu.my (I.A. Ja'e), zakaria.chemuda@newinti.edu.my (Z.C. Muda), Agusril@uniten.edu.my (A. Syamsir), chiemela.victor@uniten.edu.my (C.V. Amaechi), hmujiabah@tu.edu.sa (H. Almujibah), a.elheber@tu.edu.sa (Ali.E.A. Elshekh), Mobashir@tu.edu.sa (M.O. Bashir), a.almaliki@tu.edu.sa (A.H. Almaliki).

<https://doi.org/10.1016/j.cscm.2025.e04240>

Received 12 August 2024; Received in revised form 16 December 2024; Accepted 9 January 2025

Available online 10 January 2025

2214-5095/© 2025 The Authors. Published by Elsevier Ltd. This is an open access article under the CC BY-NC-ND license (<http://creativecommons.org/licenses/by-nc-nd/4.0/>).

limitations as well as the potential of utilising OPS in fibre-reinforced lightweight suspended concrete slabs and other impact-resistant constructions.

1. Introduction

Considerable research has been dedicated to exploring the implementation of eco-friendly green products in the construction industry through recycling agricultural waste. This approach aims to mitigate environmental pollution and promote sustainable practices in industrial waste management. The advantages and challenges associated with the utilisation of agricultural waste as construction materials, including aspects related to sustainability, environmental impact, technical performance, and economic feasibility have also been extensively debated. An example of a green product in this category is Oil Palm Shell (OPS) concrete, which combines OPS as coarse aggregate with a cementitious matrix to create an eco-friendly product. Other agricultural wastes, such as coconut shells and ash derived from byproducts and residues have shown promising performance as replacements for the conventional aggregates in concrete[1]. The oil palm plantations in Malaysia account for 41 % of the total crude palm oil production globally, resulting in significant OPS, palm oil clinker and other related byproducts[2,3]. Thus, utilising OPS as lightweight aggregates in concrete offers numerous advantages, including waste utilisation and enhanced mechanical strength. This approach also contributes to a low density, and improved thermal insulation properties of concrete, all while promoting environmental sustainability.

Previous studies have highlighted the eco-friendly significance of utilising OPS as coarse aggregate in concrete [4] [5], while also exploring the utilisation of other locally available solid waste materials such as Oil Palm Boiler Clinkers (OPBC) as coarse lightweight aggregates for the production of lightweight concrete[6,7]. The studies reported about 16 % reduction in concrete density by replacing natural aggregate with 80 % OPS. Furthermore, the incorporation of fibre into OPS concrete has been found to improve the overall performance of OPS concrete[8–10]. Specifically, the incorporation of steel fibres between 0.25 % and 1.0 % in OPS concrete yielded a significant improvement in both compressive and flexural performance [11]. The inclusion of different types of fibres in lightweight concrete has been found to enhance various engineering properties, including flexural strength, thermal shock strength, fracture toughness, impact resistance, and fatigue loadings [12–17]. Nonetheless, several factors such as the type, quantity, and characteristics of fibres, along with the water-to-cement ratio and aggregate type, can significantly influence the concrete performance [18–24].

Impact resistance is a critical property that determines the ability of concrete to withstand repeated impacts and absorb energy without developing cracks or spalling. Two categories of impacts include low-velocity and high-velocity impacts. The drop weight impact test by the ACI Committee 544 is recommended as the simplest testing method available. However, this test has limitations, such as its small sample size and test setup, which may not be suitable for assessing non-homogeneous concrete composites, non-uniform fibre distribution, reinforcement with mesh or different boundary conditions. Under Impact loading, concrete may crack on the distal face due to the propagation of reflected tensile waves from the point of impact. Even highly reinforced slabs, which possess high energy resistance, can still fail due to punching shear. Localised damage had been observed at the point of contact during an impact event, which could be attributed to compression failure near the impact point[25,26].

In a study conducted by Yew et al.,[27] explored the mechanical properties of OPS fibre-reinforced lightweight concrete and discovered that polypropylene (PP) fibres with suitable aspect ratios and geometries can enhance concrete mechanical performance. Kim et al.[9] also examined the impact resistance of OPS concrete reinforced with various types and combinations of hybrid fibres, highlighting their influence on the impact strength of the concrete. Furthermore, Islam et al.[28] found that incorporating 0.5 % steel fibres in OPS concrete significantly increased the first crack load by 1.5–3.5 times compared to fibre-free mixes. Additionally, they observed that using uncrushed OPS aggregate resulted in 15 %–152 % improvement in ultimate impact energy compared to crushed OPS aggregate mixes. In a separate study, Zamzani et al.[29] conducted experimental tests on lightweight foamed concrete reinforced with coconut fibres. Their findings highlight positive improvements in the mechanical properties of the concrete due to the inclusion of coconut fibres. Kanchidurai et al.[30] investigated the maximum impact resistance of hybrid fibre-reinforced concrete and discovered that hybridising one per cent steel fibre and one per cent glass fibre resulted in a 720 % improvement in impact resistance compared to the control specimen.

Various studies have found that adding OPS in lightweight concrete can enhance its impact resistance. Some researchers have also explored the benefits of incorporating OPS as coarse aggregates and utilising fibre reinforcement. These studies have consistently demonstrated that adding fibres can improve the impact resistance of lightweight concrete containing oil palm shells [31,32]. The study also delved into the performance of lightweight concrete slabs made with OPS and reinforced with geogrid under different support boundary conditions. They found that geogrid reinforcement led to a 29.8 % and 40.6 % increase in first and ultimate crack resistance. Anil et al. [33] also studied the support type and support layout of a bottom steel mesh reinforced with a 4 mm diameter bar at 50 mm spacing under a low-velocity impact loading. The number of blows withstood by fixed supports is higher than those with hinge supports and specimens supported on four sides had higher impact energy absorption compared to specimens supported on two supports.

The literature search conducted revealed only limited research on the impact resistance of lightweight OPS concrete reinforced with polypropylene fibres. As such, this study aims to assess the feasibility of utilising hybrid fibrillated polypropylene (PP) and PP-mesh with different support conditions. The investigation focuses on the impact of energy absorption and crack resistance at service and ultimate stages and their relationship using experimental and response surface methodology. Additionally, the study examined the specimens' ability to effectively resist cracks relative to their compressive strengths and remaining service life after impact.

This study is significant not only because the natural aggregate is entirely replaced with Oil Palm Shell (OPS) but also because it

explores the structural impact performance incorporated with varying polypropylene fibre content and boundary conditions. The findings provide valuable insights for the use of OPS concrete, particularly where impact resistance is a primary objective.

2. Materials, concrete mix design and methodology

2.1. Materials

2.1.1. Oil palm shell and polypropylene fibres

Oil palm shells (OPS), as depicted in Fig. 1(a), possess distinctive physical properties that make them an ideal replacement for conventional aggregates. They are naturally sized, with sufficient hardness while also being lighter in weight compared to traditional aggregates. This inherent lightness of oil palm shells makes OPS a suitable alternative in the production of lightweight concrete. This study used OPS within the size range of 8 mm to 10 mm.

The fibrillated propylene fibre (PPF) used is 19 mm in length and 400 MPa tensile strength, while the extruded polypropylene mesh (PPM) is made of 2 mm diameter fibre fabricated in 300 mm square consisting of 30 mm squares openings as shown in Fig. 1(b) and (c).

2.2. Concrete ingredient and mix design

In all the concrete mixes used for the production of polypropylene fibre-reinforced lightweight concrete (PPFR-LWC) with OPS, Ordinary Portland Cement complying with ASTM Type I specifications was utilised, with a consistent water-cement ratio of 0.45. Silica fume, supplied by EIKEM, having a specific gravity of 2.2 and 0.15 μm particle size was also incorporated into the mix. In addition, the dosage of superplasticiser (Sika Viscocrete-15RM) was 2 % by weight of cement, which had a specific gravity of 1.12.

The fine aggregate and OPS used had maximum particle sizes of 4.25 mm and 12.5 mm respectively as shown in the particle gradation plot in Fig. 2.

The physical properties of the fine and OPS aggregates are summarised in Table 1. The data indicates that the crushing and impact values of OPS are lower than those of natural aggregate by about 22 %, thus demonstrating a superior resistance to crushing and impact forces. This further implies that OPS exhibits an effective ability to absorb and dissipate without fracturing.

The dosages of fibrillated polypropylene fibres used are 0 %, 1 %, 2 % and 3 %. The mix design adopted in the study is presented in Table 2.

2.3. Methodology

2.3.1. Boundary conditions and fibre configurations in slabs specimen

Fig. 3(a, b, c) depicts the bottom PP fibre distribution and PP mesh configuration, along with the boundary support conditions. The slabs are simply supported at their edges with varying numbers of supports, as illustrated in Fig. 3(a). Notably, the control slab specimen as shown in Fig. 3(b) does not contain PP in the bottom layer. Conversely, the remaining samples consist of fibrillated PP randomly distributed in the bottom half of the slab, as illustrated in Fig. 3(c).

A comprehensive experiment was conducted on 36 slab specimens, each individually tested for control as well as with varying volume fractions of polypropylene fibre (PPF) at 1 %, 2 %, and 3 %. Further details of the experimental specimens are shown in Table 3. The Concrete mix designs containing 1 %, 2 % and 3 % fibre are designated as PP1, PP2, and PP3 respectively.

2.3.2. Concrete production

Before mixing, the OPS aggregates were pre-soaked in clean water for 24 h to lower initial water absorption characteristics and ensure lower porosity in the final concrete mix. Next, the cement and OPS aggregates were mixed for about 3 min before adding water and superplasticiser and continued to mix for another 5 min. The specified PP fibre content was then evenly dispersed by hand in the



Fig. 1. (a) Oil palm shell lightweight aggregates (b) Fibrillated polypropylene fibre (c) Extruded polypropylene mesh.

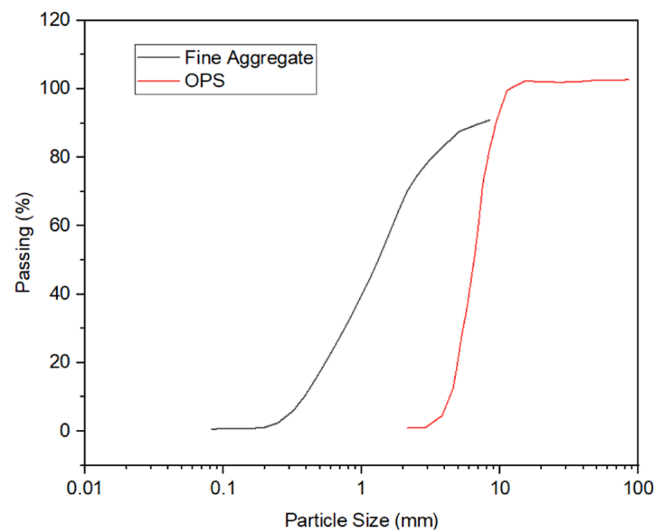


Fig. 2. Particle size distribution of fine and OPS aggregates.

Table 1

Physical properties of fine sand and OPS.

Parameter	Fine sand	Coarse aggregate - OPS
Bulk density (Kg/m ³)	1500–1550	568
Specific gravity	2.45	1.3
Fineness modulus	1.4	6.08
Loss Angeles abrasion value (%)	-	4.90
Aggregate impact value (%)	-	7.51
Aggregate crushing value (%)	-	8.00
24-h water absorption	3.89	23.0

Table 2

Concrete mix design.

Mix Code (Fibre)	Binder		Aggregate		PP Fibre (%)	w/c	SP %	Slump (mm)	Oven Dry Density (kg/m ³)
	Cement (kg)	Silica Fume (%)	OPS (kg)	Sand (kg)					
Control	530	5	200	795	0	0.4	2	130	1905
PP1	530	5	200	795	1	0.4	2	75	1825
PP2	530	5	200	795	2	0.4	2	45	1700
PP3	530	5	200	795	3	0.4	2	20	1580

mixture and mixed for an additional 4 min to ensure uniform distribution. The specimens were cast in lubricated timber formworks as shown in Fig. 4(a) and left to cure for 24 h before being de-moulded and submerged in a bath of clean tap water for a total of 28 days. The specimen surfaces were whitewashed with paint to allow for easier identification of cracks during testing as shown in Fig. 4(b).

2.3.3. Experimental procedure

2.3.3.1. Compressive strength test. The 28-day compressive strength of the concrete was evaluated through a compressive strength test performed on 150 * 150 * 150 concrete cubes, utilising the Universal Testing Machine at the Civil Engineering Department of Universiti Tenaga Nasional, Malaysia. The samples were cured in clean portable water at room temperature and for each fibre content, three cubes were prepared to calculate the average compressive strength. The compressive load was gradually and uniformly applied to each specimen within the range of 0.15 – 0.35 MPa/s to ensure accurate measurement.

2.3.3.2. Low-velocity impact test. The low-velocity drop-weight impact test was adopted in this study, where a steel ball weighing

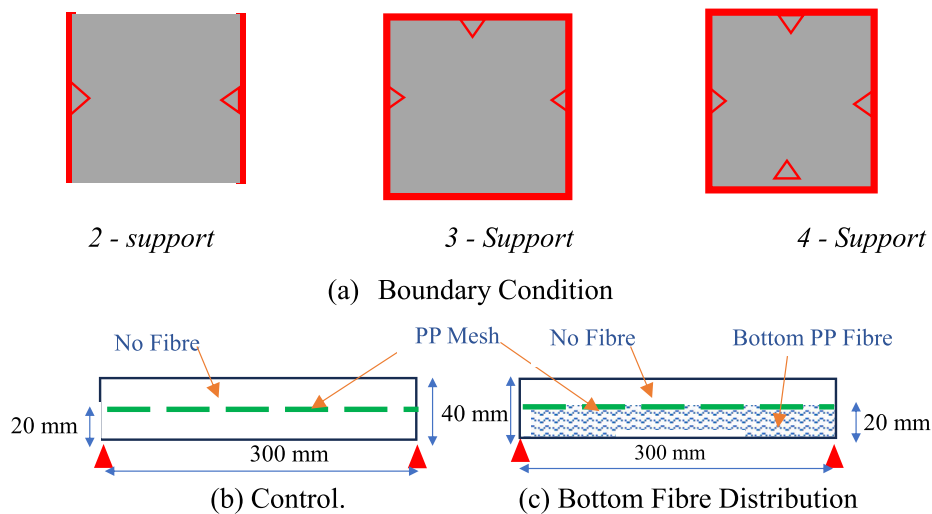


Fig. 3. Illustrations of boundary conditions and fibre configurations.

Table 3

Specifications of test specimens.

Mix code	PP fibre (%)	PP mesh	Boundary conditions	No slab specimen tested
Control 1	0 %	Yes	2-way	3
Control 2	0 %	Yes	3- way	3
Control 3	0 %	Yes	4- way	3
PP1-1	1 %	Yes	2-way	3
PP1-2	1 %	Yes	3-way	3
PP1-3	1 %	Yes	4-way	3
PP2-1	2 %	Yes	2-way	3
PP2-2	2 %	Yes	3-way	3
PP2-3	2 %	Yes	4-way	3
PP3-1	3 %	Yes	2-way	3
PP3-2	3 %	Yes	3-way	3
PP3-3	3 %	Yes	4-way	3

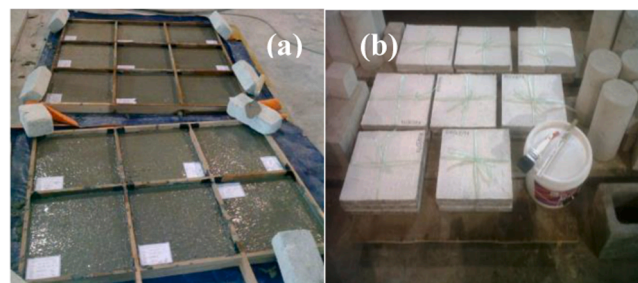


Fig. 4. Slab specimen preparation (a) Slab formwork (b) Slab specimen with whitewash applied.

1.05 kg was dropped from a height of 0.3 m onto a specimen measuring 300 mm × 300 mm × 40 mm. Each of the specimens was mounted on a specially manufactured rectangular steel rack frame and simply supported on sides as shown in Fig. 5. In each case, the number of blows at the initial crack and failure was recorded as well as the total crack lengths, width and crack depths at the service (first) crack and ultimate (failure) crack were measured using a filler gauge. Each data point was an average of three (3) specimen readings.

The potential energy due to the drop of the weight on the specimen was absorbed as strain energy, generating stresses that cause cracks in the target element. The width, depth, and length of the crack developed and its failure mode were recorded and the associated amount of energy absorbed and the crack resistance were computed.

2.3.3.3. *Computation of impact and crack resistance parameters.* Eqs. 1–3 describe the relationship between the potential energy of the



Fig. 5. Illustration of impact test arrangement using impact test rig.

drop-weight projectile and the strain energy dissipated during crack development.

$$e = m * g * h \quad (1)$$

$$E_s = N_s * e \quad (2)$$

$$E_u = N_u * e \quad (3)$$

The variables involved include energy per blow (e) in Joules, the mass of steel ball (m) in kg, and $g = 9.81 \text{ m/s}^2$. The height of the drop of a steel ball (h) is measured in metres, E_s is the service impact energy (J), and E_u is the ultimate impact energy (J). N_s represents the number of blows at the first crack (service) and N_u is the Number of blows at the failure (ultimate) crack.

The service and ultimate Crack resistance were calculated using Eqs. 4 and 5, respectively, as proposed by Kankam[34].

$$R_s = E_s / (l_c * d_c * W_c) \quad (4)$$

$$R_u = E_u / (l_c * d_c * W_c) \quad (5)$$

where R_s is Service crack resistance (N/mm^2), R_u = ultimate crack resistance (N/mm^2), l_c = total length of all cracks (mm), d_c = maximum crack depth (mm) and w_c = maximum crack width (mm).

An additional factor that is analysed is the crack resistance ratio, which is the ratio of crack resistance to the compressive strength of the concrete. This metric evaluated the effectiveness of the crack resistance against its compressive strength.

The service and ultimate impact crack resistance ratio are computed through Eqs. 6 and 7.

$$Cr_s = R_s / f_{cu} \quad (6)$$

$$Cr_u = R_u / f_{cu} \quad (7)$$

Where, Cr_s = Service Impact crack resistance ratio, Cr_u = Service Impact crack resistance ratio, R_s = Service crack resistance (N/mm^2), R_u = ultimate crack resistance (N/mm^2), f_{cu} = cube compressive strength.

Furthermore, to easily evaluate quantitatively the improvement in the impact resistance characteristics; the impact residual strength ratio (I_{RS}) was formulated as the ratio of ultimate impact energy to service impact energy as given in Eq. 8 [35].

$$I_{RS} = E_u / E_s \quad (8)$$

Where I_{RS} represent the Impact residual strength ratio, E_s is the service impact energy (J), and E_u is the ultimate impact energy (J).

The impact residual strength ratio helped to evaluate the post-crack behaviour of the composites easily and could also be taken as a measure of the ductility of the composite imparted by the fibre incorporated into the matrix.

3. Response surface analysis

Response surface methodology (RSM) is a highly effective approach widely used across various fields today. It encompasses a set of mathematical and statistical techniques used for experimental design, modelling, evaluating the impact of multiple variables, and optimisation [36]. Conventionally, this methodology relies on experimental data, but observational data as an alternative are also considered[37]. Some of the software used for response surface analysis includes XLSTAT, Minitab and design expert software. For this study, Version 13:2021 of Design-Expert is in this study because of the flexibility. The interactions between factors and responses are depicted in the form of contours and 3D response surfaces to illustrate the relationship.

The central composite design based on 2-factorial designs was employed for its adaptable design structure to accommodate custom

models. The factors considered are the boundary conditions (i.e., supports) and polypropylene fibre (PPF) content, while the responses include service and ultimate impact energy absorption and crack resistance. Each combination includes, 2, 3 and 4 supports with 1 %, 2 % and 3 % PPF respectively. The results are further analysed using ANOVA and diagnostic results.

Depending on the relationship between the response(s) and factors, linear, quadratic cubic, etc models are suggested as shown in Eqs. (9) and (10).

$$f = A_0 + A_1x_i + A_2x_{ii} \dots A_nx_n + \varphi \quad (9)$$

Where f and x are the factor and variable respectively. Also, A_0 is the intercept at $x_i = x_j = 0$, A is the coefficients.

$$f = A_0 + \sum_{i=1}^n A_i x_i + \sum_{i=1}^n A_{ii} x_i^2 + \sum_{i=1}^{n-1} \sum_{j>1}^n A_{ij} x_i x_j + \varphi \quad (10)$$

Where i and j denote linear and quadratic encrypted quantities, and n is the numerical variable.

The ANOVA result of each analysis establishes the mean variability between the impact energy and crack resistance of the lightweight concrete specimens through the measure of statistical significance by ensuring a 95 % confidence level, a statistical significance of $p - value \leq 0.05$. In each case the $p - values$, *lack of fits*, *standard deviations*, and variations between adjusted and predicted coefficient of determinations (R^2_a and R^2_p) are evaluated.

4. Results and discussion

Details of experimental impact test results and analysis for the impact energy, crack resistance, crack resistance ratio and impact residual strength are discussed in this section.

4.1. Compressive strength

Fig. 6 indicates the variation in compressive strength of lightweight OPS concrete reinforced with varying polypropylene fibre volume fractions.

A noticeable decrease in compressive strength of between 14 % and 35 % compared to the control sample is observed, suggesting the negative impact on compressive strength with a higher Polypropylene fibre dosage when natural aggregate is completely replaced with OPS. Several factors contribute to this phenomenon. Notably, as the PPF increases, the surface area within the concrete mix also increases, necessitating a greater amount of paste requiring a higher water-cement ratio, which can ultimately affect the overall compressive strength. Other specific issues include firstly, the fibre-to-fibre interaction impedes the cement paste flow, leading to localised stress concentrations and consequent crushing of the OPS. sly, a high fibre dosage can result in a balling effect, creating voids and weakening the bond between the fibres and the cement paste. Lastly, low workability can make it difficult to ensure proper fibre distribution and orientation throughout the concrete at higher fibre dosages, decreasing load transfer efficiency and compressive strength. A similar trend in declining compressive strength with the introduction of OPS has been reported [38,39].

4.2. Prediction models

To further investigate the performance of the lightweight concrete, additional responses were predicted for specimens with up to 8 supports and containing up to 5 % polypropylene fibre content. The regression models are developed from the experimental results for the prediction of service impact energy absorption (E_s), ultimate impact energy absorption (E_u), service crack resistance (R_s), and ultimate crack resistance (R_u) and are shown in Eqs. 11- 14. Where A and B represent supports and polypropylene fibre respectively. The equations, which are based on the actual factors were used to predict additional responses with varying ranges of factors.

$$E_s = -71.38 + 47.792A + 65.24B \quad (11)$$

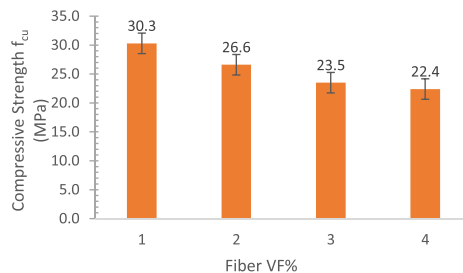


Fig. 6. Variation of 28-day OPS concrete compressive strength with different PPF content.

$$Eu = -127.696 + 155.327A - 54.321B + 73.178 + AB \quad (12)$$

$$Rs = -55.74 + 37.35A + 319.59B + 24.85AB + 5.89A^2 - 81.49B^2 \quad (13)$$

$$Ru = -108.6618 + 73.525A + 523.0717B + 40.05AB + 4.675A^2 + 129.1417B^2 \quad (14)$$

4.3. Impact energy absorption

Figs. 6 and 7 compare the combined correlational influence of boundary conditions and polypropylene fibre on service and ultimate impact energy of lightweight concrete slabs.

4.3.1. Experimental impact energy absorption under service loading

Fig. 7(a) reveals a general increase in service impact energy in direct proportion to the increasing boundary conditions and fibre content. The service impact energy shows a significant improvement of between 2.6 and 3.3 times for specimens with 2 supports, 2–2.4 times for specimens with 3 supports and 1.8–2.2 times for 4 supports when fibre content increases between 1 % and 3 % with a maximum energy of 457.4 J recorded in specimen containing 3 % polypropylene fibre and supported on 4 supports. The findings also emphasise the significant contribution of fibre content to the specimen impact energy, particularly at 1 % with 78 %, 90 % and 164 % increased for 4, 3 and 2 supports respectively compared to the control specimen. Fig. 7(b) further demonstrates the percentage increases in impact energy for each boundary condition with increasing fibre content, indicating a higher rate of improvement in specimens with fewer constraints. Several studies have reported similar improvements in the impact resistance of oil palm shell concrete, specifically, Yahaghi [25] reported significant improvement at 0.3 % fibre content for 30 mm concrete under service loading. Muda, et al. [40] also reported improved impact and crack resistance with an increased section thickness of oil palm shell concrete.

4.3.2. Predicted impact energy absorption under service loading

To further explore the influence on the impact resistance of lightweight concrete with increased boundary conditions and fibre content, additional responses were predicted for specimens with 8 supports and containing up to 5 % polypropylene fibre content. The 2D contour and 3D response surface plots in Fig. 8(a) and (b) illustrate the predicted cubic responses. The results indicate improvement beyond the experimental findings with an increased number of supports and fibre content. The contour lines and colour gradings reveal the fibre content in cases with up to 4 supports does not significantly influence the impact energy absorption at the service stage (E_s) while fibre content of between 1 % and 2 % causes a decrease in the performance in cases with more than 5 supports. Generally, a volume fraction of polypropylene fibre above 4 % works sufficiently well will all support cases, with the maximum performance of 780 Joules exhibited in the case having 8 supports with 5 % fibre content. This is equivalent to about 3.3 times the maximum energy absorption (234 joules) exhibited by the control sample with 4 supports without fibre. Detailed predicted data can be referred to in the Appendix.

4.3.3. Experimental impact energy absorption of OPS concrete under ultimate loading

Fig. 9(a) illustrates the impact of boundary conditions and volume fractions of polypropylene fibre content on the ultimate impact energy of the OPS slab concrete. The enhancement in ultimate impact energy is in the same trend as the service impact energy, reaching a peak value of 1194 J in the specimen containing 3 % fibre with 4 supports. This represents a 167 % improvement compared

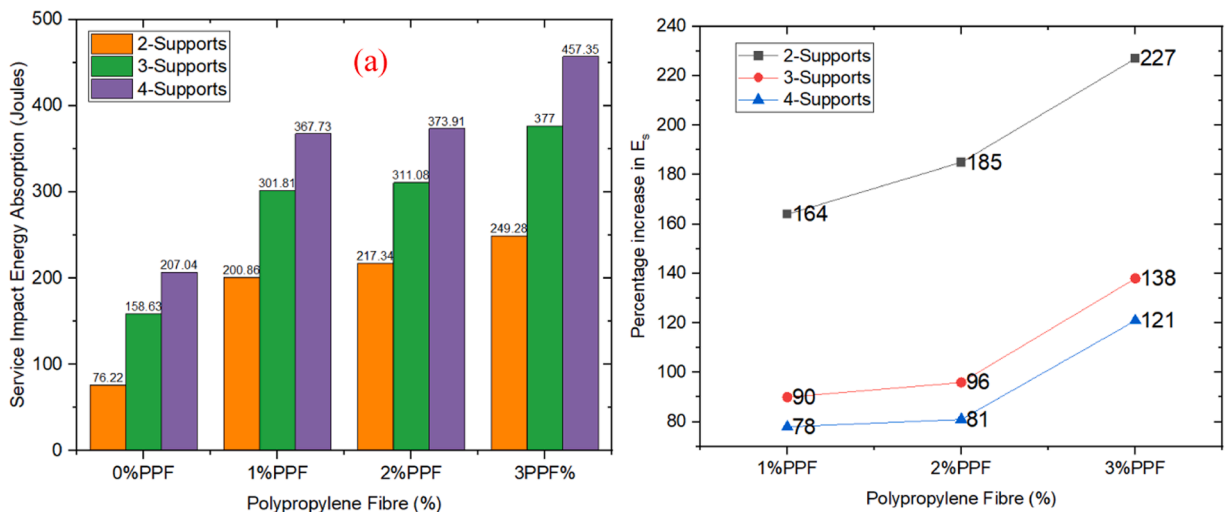


Fig. 7. (a) Experimental service impact energy absorption of OPS concrete slab (b) Percentage increase in service impact energy.

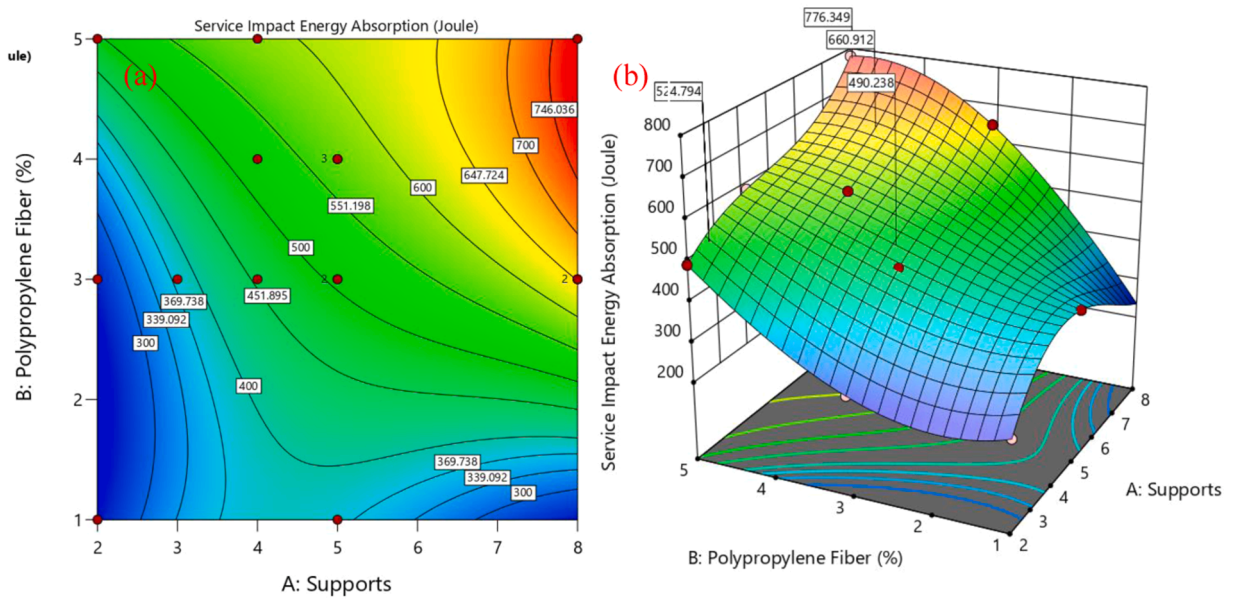


Fig. 8. Correlational influence of predicted service impact energy absorption of OPS concrete slab with varying boundary conditions and fibre content (a) 2D contour plot (b) 3D response surface plot.

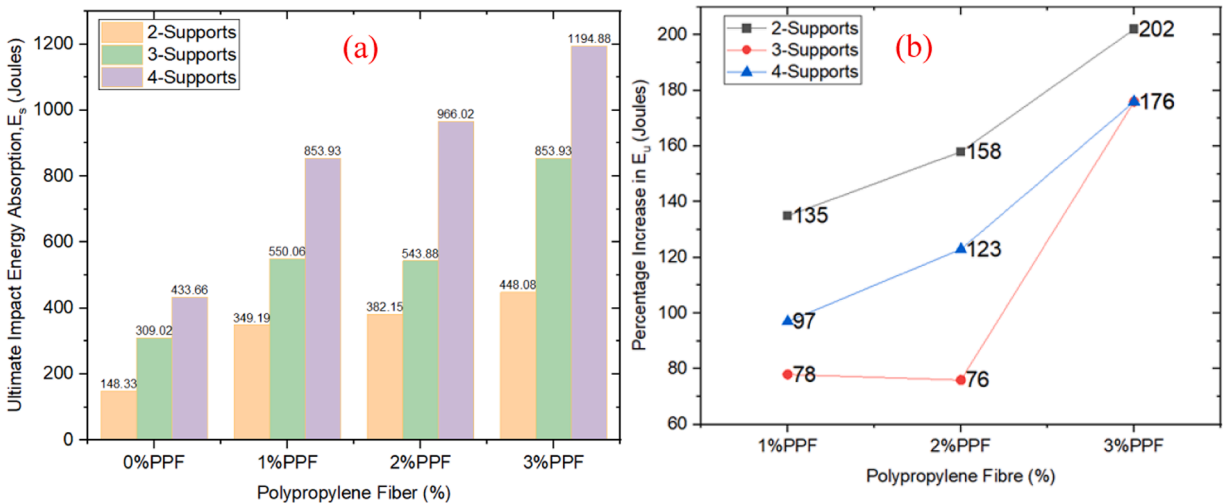


Fig. 9. (a) Experimental ultimate impact energy absorption of lightweight-OPS concrete slab (b) Percentage increase in ultimate impact energy.

to the control sample with equal support. Variations in the impact energy with varying fibre content and different boundary conditions are shown in Fig. 9(b). The substantial improvement of the OPS concrete at 1 % fibre content, ranging from 78 % to 135 %, followed by 3–22 % as fibre content increases to 2 %, and finally to 40 % with 3 % fibre content for 2, 3 and 4 supports respectively is evident. This improvement is related to the low impact and crushing value of OPS and the higher tensile strength of the PPF. Similar findings were also reported in terms of improved impact and crack resistance [25,40]. Mo et al., [41] also reported improved impact resistance and crack width of oil palm shell concrete with the introduction of hybrid steel fibres.

Fig. 10 illustrates the predicted results of cases containing 8 supports and up to 5 % fibre content. The 2D contour plot, reveals significant improvement in the ultimate impact energy absorption with a higher number of supports. Most importantly, the number of supports exhibits more influence on this parameter. Similar to the trend observed in the experimental results, the highest performance of 3770 Joules is recorded with 8 supports and 5 % polypropylene, indicating about 9 times the performance of the control sample with 4 supports.

The observed improvement in impact energy absorption as shown is two-fold, one is due to the low crushing and Impact values of the OPS together with the combined influence of fibrillated and mesh polypropylene fibres due to their high tensile strength. Thus, as

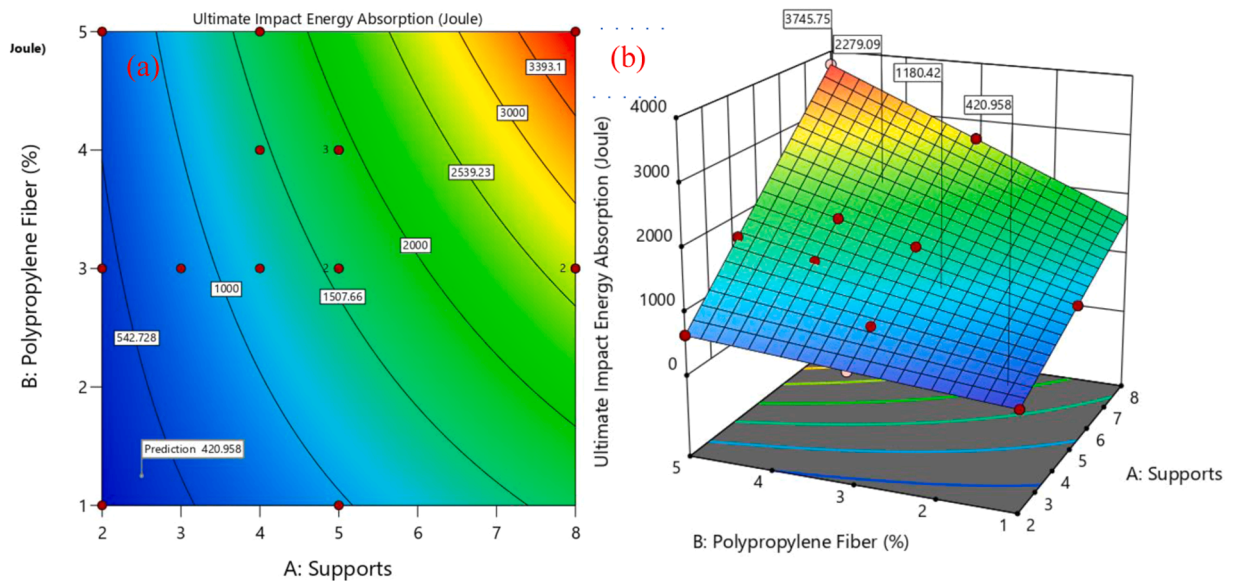


Fig. 10. Correlational influence of predicted ultimate impact energy absorption of OPS concrete slab with varying boundary conditions and PPF content (a) 2D contour plot (b) 3D response surface plot.

the fibre dosage increases, the fibre network becomes denser, and the bridging effect across cracks improves, resulting in higher impact energy absorption. s , is the efficient load distribution in all directions with a higher number of supports. This combined contribution enhanced the minimisation of strain accumulation with consequent damage accumulation and propagation. This distributes the impact load over a larger area, allowing enhanced energy to be absorbed by all supports. Furthermore, OPS are known to act as stress concentrators, leading to localised microcracks. Detailed predicted data can be referred to in the Appendix.

4.4. Crack resistance

Figs. 11 and 12 present a comparison of the combined correlational effects of boundary conditions and polypropylene fibre content on the service and ultimate crack resistance of lightweight polypropylene fibre-reinforced concrete.

4.4.1. Experimental crack resistance of OPS concrete under service loading

Fig. 11(a) demonstrates a consistent increase in service crack resistance across all specimens as the boundary conditions (supports) and fibre content increase. A significant improvement in crack resistance is exhibited with increasing PP fibre content, with the highest

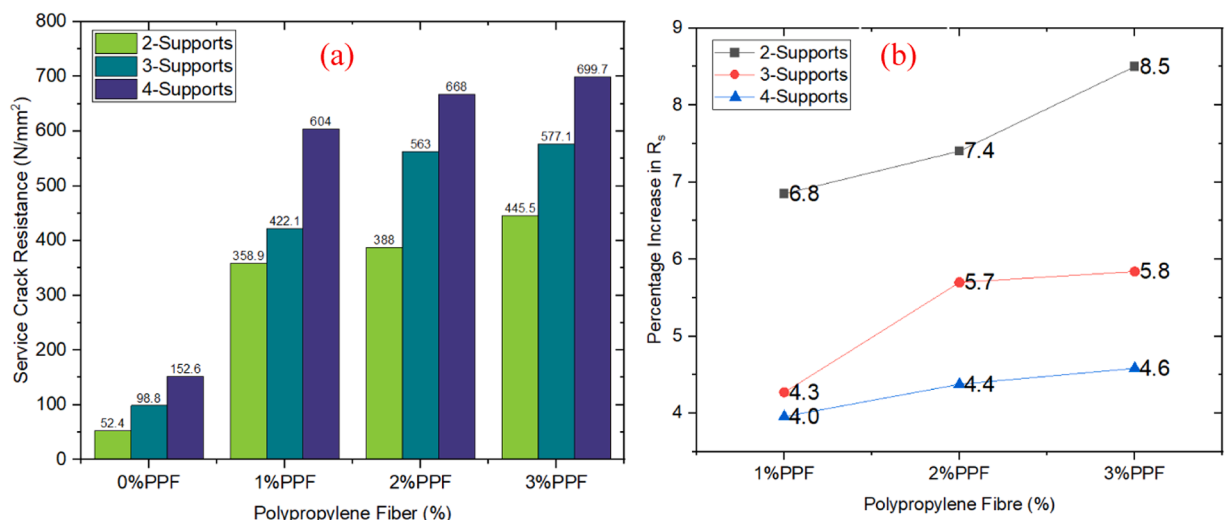


Fig. 11. (a) Experimental service crack resistance of lightweight-OPS concrete slab (b) Percentage increase in service crack resistance.

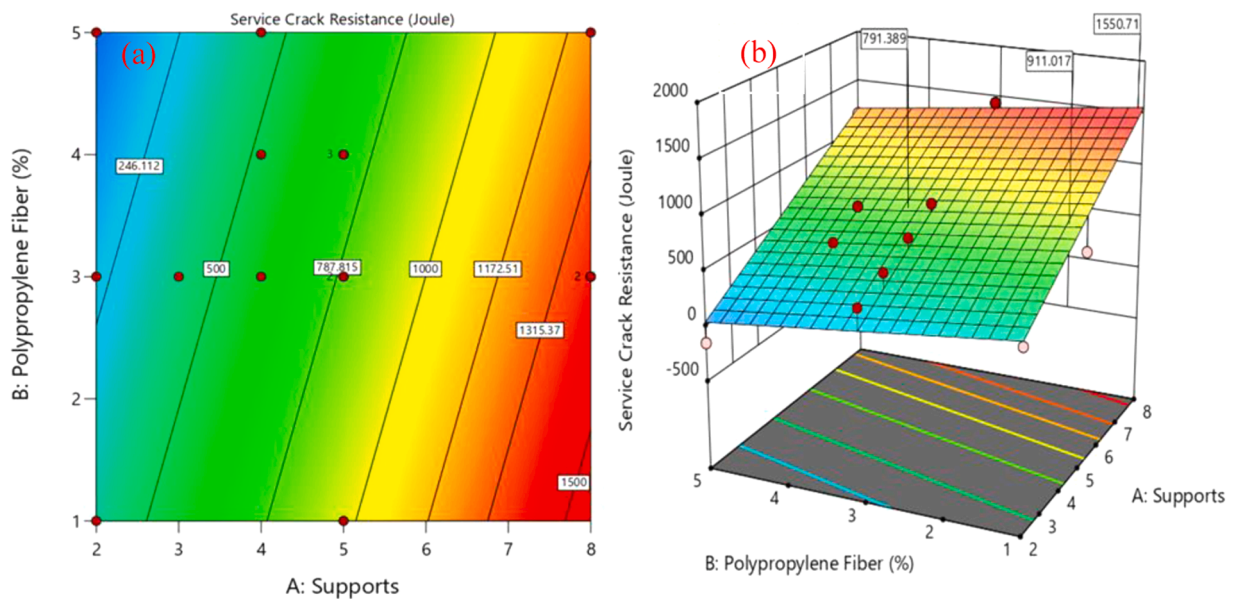


Fig. 12. Correlational influence of predicted service crack resistance of OPS concrete slab with varying boundary conditions and fibre content (a) 2D contour plot (b) 3D response surface plot.

levels observed in specimens with 2 supports ranging between 585 % and 750 %, followed by 327–484 % for 3 supports and 296–359 % for specimens with 4 supports. Similarly, an increase in the number of supports results in improved crack resistance. Additionally, Fig. 11(c.) compares the crack resistance variation of the specimen with the control sample, showing a remarkable improvement in the specimen with 2 supports. Nonetheless, the maximum service crack resistance of 700 J was exhibited by a specimen containing 3 % fibre and supported on 4 supports.

4.4.2. Predicted crack resistance under service loading

Fig. 12 a and b demonstrate the improvement in the crack resistance of all specimens with increasing supports and fibre content.

With exceptions in decline performance in cases with up to 3, and 5–8 supports specimens containing fibre content beyond 2 % and 3 % respectively as observed with diminishing green colour to blue in the case of 2 and 3 supports, and from red to yellow in the case of 5–8 supports. The optimal crack resistance was exhibited by a specimen with 8 supports with fibre content up to a maximum of 4 %. Detailed predicted data can be referred to in the Appendix.

4.4.3. Experimental crack resistance OPS concrete under ultimate loading

Fig. 13(a) highlights the variation of ultimate crack resistance (R_u). Although the trend exhibited is similar to the service crack

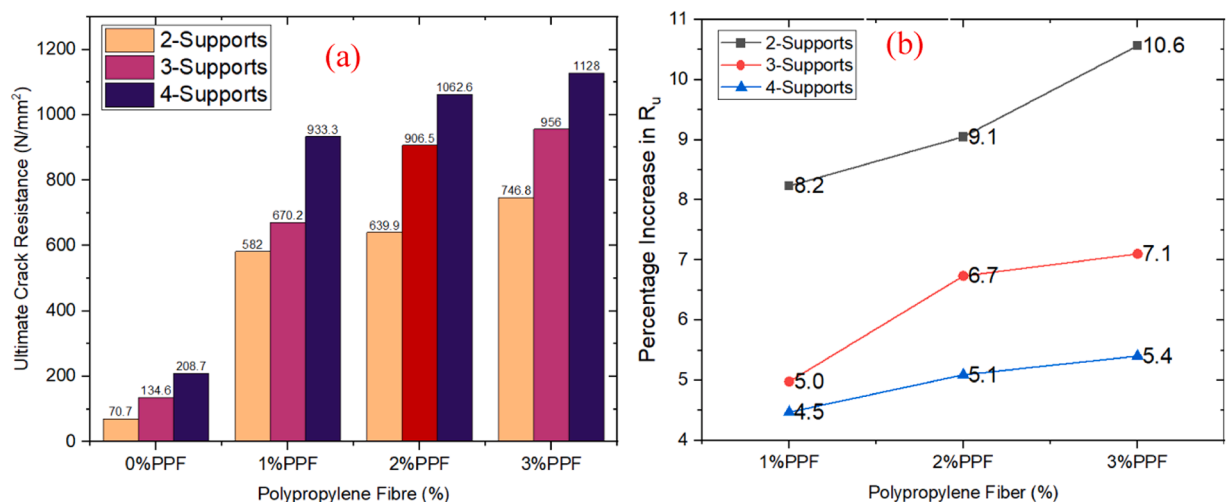


Fig. 13. (a) Experimental ultimate crack resistance absorption of lightweight-OPS concrete slab (b) Percentage increase in ultimate crack resistance.

resistance, as envisaged the ultimate values were all higher than the service cracks with the highest value of 1128 N/mm^2 exhibited by the specimen containing 3 % polypropylene fibre and supported on 4 supports. This improvement is about 5.4 times the control sample in that group, which infers the general contribution of the PPF to the performance of the OPS concrete. A detailed percentage difference in R_u for each support with varying volume fractions of fibre is demonstrated in Fig. 13(b). The variation in crack resistance at this stage is attributed to the ability of the PP fibre to control micro-cracks at the initial phase, as well as the bridging capability of the polypropylene mesh to address minor cracks at the failure phase. Additionally, the different support conditions may have influenced the distribution of impact energy and the formation of failure zones within the specimens, leading to varying performance outcomes. Al-Rousan et al., [42] have reported similar improvement in the two-way slab at 0.9 % polypropylene fibre, and another study reported improvement in energy absorption of concrete with polypropylene fibre [43].

4.4.4. Predicted crack resistance under ultimate loading

Based on the predicted responses depicted in Fig. 14, the variation in ultimate crack resistance is represented by a gradual colour change from blue to red, with blue indicating the lowest and red representing the highest resistance. The decrease in ultimate crack resistance observed in cases with 2 and 3 supports containing polypropylene fibre, as shown in Fig. 14(a), is attributed to the decline in specimen ductility caused by fibre clumping, leading to poor fibre distribution and consequent reduction in crack bridging, energy absorption, and crack resistance. Another possibility could be interfacial bonding, which might have resulted in premature fibre pullout, further affecting crack resistance. Similarly, in cases with more than 5 supports, crack resistance decreases with higher fibre content. Nonetheless, beyond this point, crack resistance is observed to improve in direct proportion to both supports and fibre content. Detailed predicted data can be referred to in the Appendix.

4.4.5. Fit statistics and diagnostic analysis

The fit statistical results for service and ultimate impact energy returns p -values of less than 0.05 which is significant, with the difference between the adjusted and predicted coefficient ($AdjR^2 - AdjR^2$) maintained at a satisfactory value of less than 0.2 which is based on the guidance provided by the design expert software manual. This indicates that all predicted values are in reasonable agreement with the adjusted coefficient of determination. A summary of the fit statistics results is shown in Table 4. The diagnostic analysis including normal plots of residuals, residuals vs Run and plots of predicted and actual responses are within specified limits.

4.4.6. Relationship between Impact energy and crack resistance

Fig. 15 (a and b) illustrate the relationship between Impact energy absorption and Crack resistance of the lightweight-OPS concrete specimens at service (E_s and R_s) and ultimate stage (E_u and R_u) respectively. Fig. 15(a) reveals optimum crack resistance at 3 % fibre content with all number of supports at the service stage. The crack resistance (R_s) is observed to drop beyond 3 % with the lowest observed at 5 % fibre content as seen in experimental runs 2SPT-5 %PPF, 4SPT-5 %PPF, 5SPT-5 %PPF, 6SPT-5 %PPF. This performance is attributed to the proper distribution and anchorage of fibre with the concrete matrix.

On the other hand, crack resistance is predominantly lower at most of the impact energy absorption levels as observed in Fig. 15(b). This trend is attributed to the impact load exceeding the bearing capacity of both oil palm shell aggregate and polypropylene fibres, thereby resulting in reduced crack resistance. This is similar to the compressive behaviour demonstrated in Fig. 6. Furthermore, Ja'e et al. have established a similar relationship between impact energy and compressive strength[44].

4.5. Failure modes of lightweight concrete specimens

The failure mode of fibres can manifest in various patterns, depending on factors such as impact energy, boundary conditions, fibre content and slab thickness. When a concrete specimen is subjected to an impact load on its frontal face, cracks may develop along with potential spalling on the distal face (bottom). This occurs due to the propagation of reflected tensile waves from the point of impact. The point of contact on the frontal face also sustains localised damage, likely caused by compression failure resulting in concrete crushing. Typically, cracks originate from the centre and propagate towards the edge of the distal face under tensile stress. As a failure crack approaches a fibre, the anticipated path of the crack creates tensile stresses that may lead to either tensile failure or pull-out of the fibre due to debonding at the interface between the fibre and the concrete matrix. Upon reaching the fibre-matrix interface, the stress concentration at the crack tip diminishes, effectively halting further crack propagation. This phenomenon is commonly known as the bridging effect- the ability of fibre-reinforced concrete to prevent crack spreading by connecting the crack faces[45–47]. As load increases, the PP fibres within the concrete eventually fail through complete pullout and tensile failure while the PP mesh elongates to prevent total collapse.

The representation in Fig. 16 is based on the optimal experimental fibre content. The specimen crack patterns are tagged using specific codes for easier interpretation. For example, 2S-0 %@S where 2S represents the number of supports, 0 % fibre volume fraction and @S, represent the crack stage, i.e., 'service' while in other cases @U stands for 'ultimate'.

When compared to OPS concrete containing only PPF mesh, specimens containing polypropylene fibre can be seen to have exhibited significant improvement of 238 %, 126 % and 113 % in crack resistance at the service stage and corresponding 215 %, 139 % and 170 % at the ultimate stage in specimens with 2 supports, 3 supports and 4 supports respectively. In all cases, at the service stage, cracks are visible at distal faces parallel to the supports with the number of segmental zones equivalent to the number of supports with local crushing damage at the ultimate stage. The propagation of cracks relative to the restrained ends is attributed to stress concentration near the supports. Generally, specimen performance at service and ultimate stage are at optimal 2 supports (see 2S-3 %

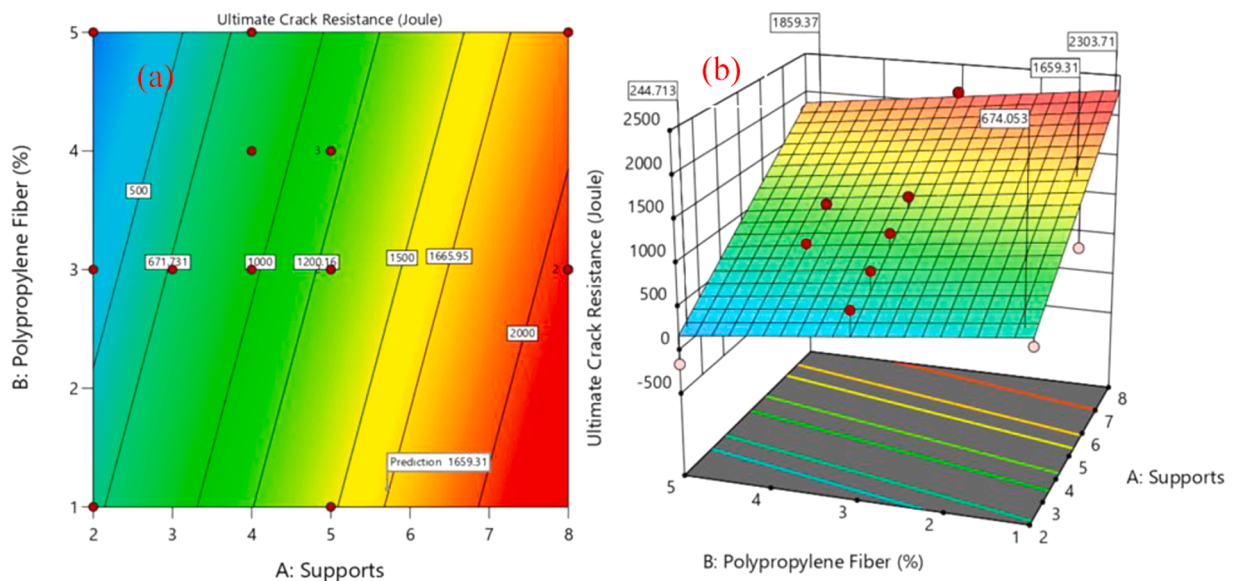


Fig. 14. Correlational influence of predicted ultimate crack resistance of lightweight concrete slab with varying boundary conditions and fibre content (a) 2D contour plot (b) 3D response surface plot.

Table 4

Comparison of fit statistical data of response model.

	E_s	E_u	R_s	R_u	Remarks
Model Type	Cubic	2FI	Linear	Linear	Suggested
A	< 0.0001	< 0.0001	< 0.0001	< 0.0001	Significant
B	< 0.0001	< 0.0001	0.0216	0.0449	Significant
AB	< 0.0001	< 0.0001	-	-	Significant
A ²	< 0.0001	-	-	-	Significant
B ²	< 0.0001	-	-	-	Significant
A ² B	< 0.0001	-	-	-	Significant
AB ²	< 0.0001	-	-	-	Significant
A ³	< 0.0001	-	-	-	Significant
B ³	< 0.0001	-	-	-	Significant
Std. dev	0.8468	7.7	147.62	233.85	Significant
R ²	1.0000	0.9999	0.8902	0.8680	
Adjusted R ²	1.0000	0.9999	0.8733	0.8477	Significant
Predicted R ²	0.8901	0.9999	0.7928	0.7508	Significant

@S and U) and continue declining with increased boundary conditions as demonstrated in specimens 3S-3 %@U and 4S-3 %@U. This indicates that an increased number of restraint conditions significantly affect specimens' ductility. Notably, specimens without fibre exhibit complete segmental failures contrary to what was observed in the fibres where failed segments are still completely segmental failures where the failed segments remained in position. Furthermore, specimens with high fibre dosage showed local compressive damage at the frontal point of contract, while those with low fibre dosage exhibited local crushing and shear cracks. These observations were made under the condition of ultimate cracks.

The cracks resulting from impact loading in the slab specimens, as illustrated in Fig. 17 (a), show a 17 % and 13 % decrease in average length with the incorporation of up to 2 % polypropylene fibre (PPF) in specimens with two and four supports. This reduction is sustained even when the PPF content is increased to 3 % in the simply supported slab. In contrast, the crack length increases in specimens with 3 and 4 supports. This inferred that the inclusion of PPF in OPS does not contribute much to the control of crack length and width. Moreover, it is observed that the crack lengths tend to predominantly increase with an increase in the number of supports. This suggests that a higher number of restraints in the specimen leads to a greater impact on the structure and subsequent dissipation of strain energy, resulting in localised fractures and crack formation. On the other hand, Fig. 17 (b) indicates no variation in crack width, maintaining a constant crack width of 2 mm regardless of the number of supports or fibre content. In a study, Kankam[34], reported similar improvement in impact and crack resistance performance in palm kernel fibre-reinforced concrete with an increased dosage of polypropylene fibre.

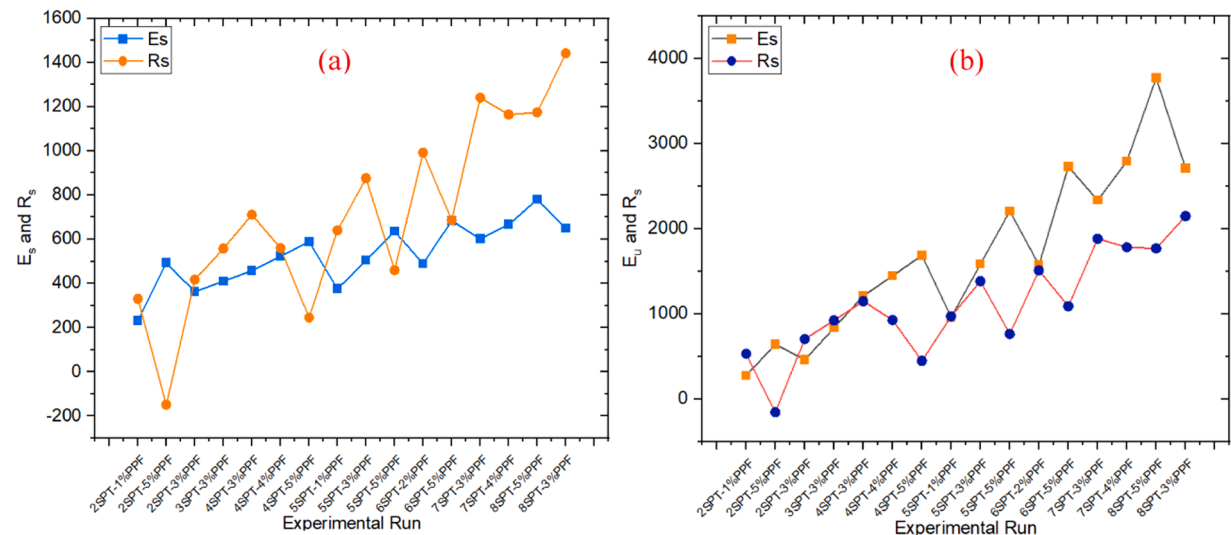


Fig. 15. Relationship between Impact energy absorption and crack resistance of OPS concrete (a) at service state (b) at the ultimate state.

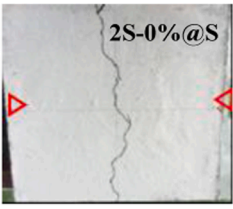
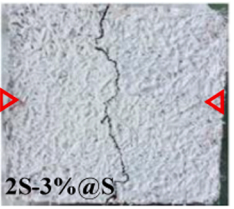
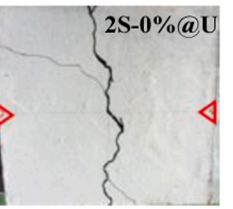
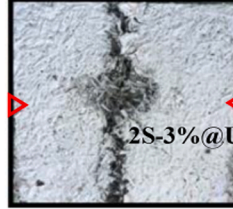
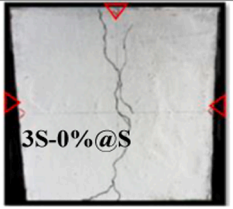
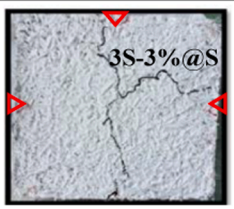
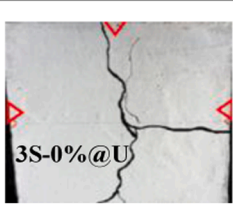
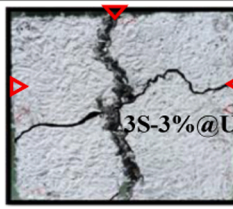
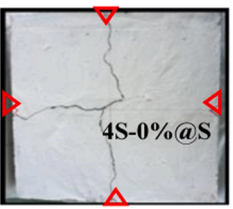
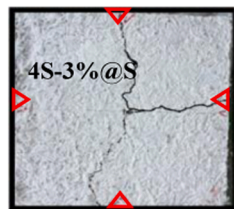
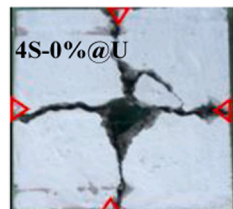
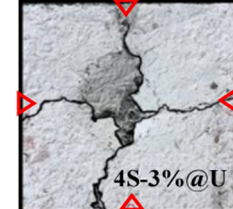
	Service Cracks		Ultimate cracks	
	0% PPF	3% PPF	0% PPF	3% PPF
2-supports				
	N(s) = 24	N(s) = 81	N(u) = 46	N(u) = 145
3-supports				
	N(s) = 54	N(s) = 122	N(u) = 102	N(u) = 244
4-supports				
	N(s) = 69	N(s) = 147	N(u) = 143	N(u) = 386

Fig. 16. Failure modes OPS concrete at service and ultimate impact loadings.

4.6. Crack resistance ratio

Fig. 18 illustrates the relationship between the polypropylene fibre volume fraction and the crack resistance (Cr) ratio at service and ultimate failure conditions for each support condition. The Cr ratio serves as a measure of how effectively a material resists

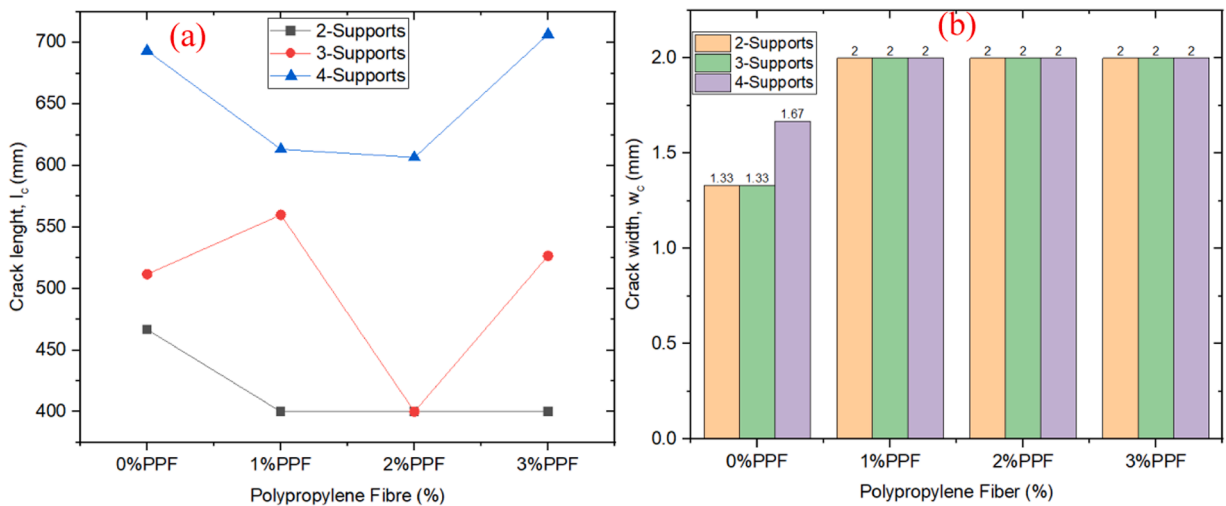


Fig. 17. Effect of PPF content and boundary conditions on (a) crack length (b) crack width.

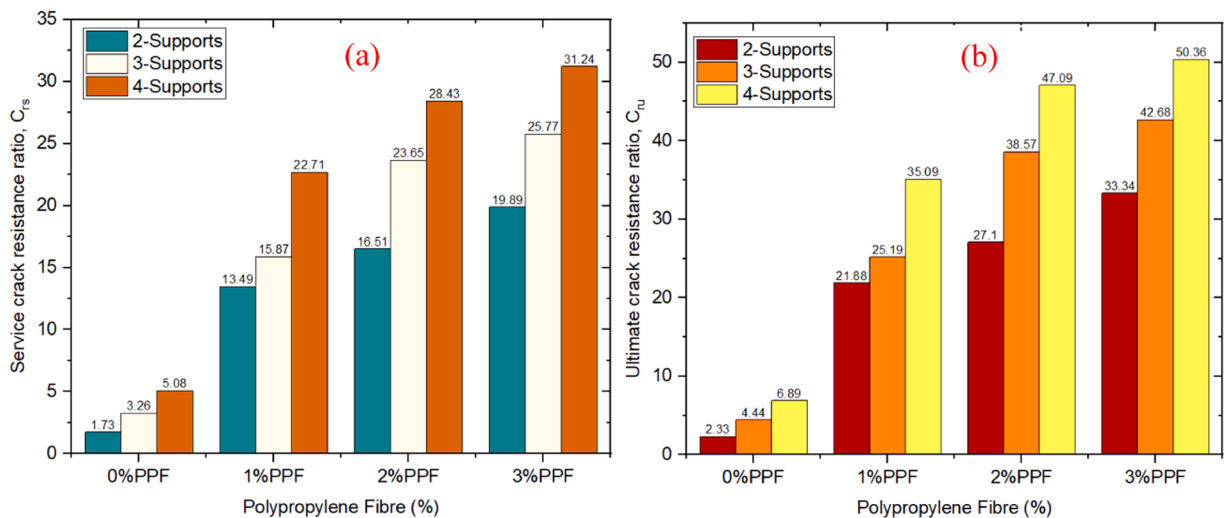


Fig. 18. Comparison of service and ultimate crack-resistant ratios of OPS concrete with varying boundary conditions and fibre dosage.

cracking relative to its compressive strength. Notably, both service and ultimate Cr ratios demonstrate an increase as the number of supports and fibre dosage increases, thereby indicating the contribution of PPF in how OPS concrete resists concrete with respect to its compressive strength. Yew et al. [48] reported a similar improvement in the crack resistance of polypropylene fibre-reinforced oil palm shell concrete. Also, Loh et al. [49] specifically highlighted the improvement in the crack resistance ratio of an oil palm shell lightweight concrete with 0.4 % polypropylene fibre.

4.7. Impact residual strength ratio

Fig. 19 shows the correlation between the impact residual strength ratio (I_{RS}) against the fibre volume fraction for each boundary support condition. This I_{RS} provides valuable insight into the ability of each specimen to retain its strength or remaining service life, following impact loading. In each of the cases considered, the I_{RS} tend to slightly increase as the fibre content increases. This performance is however indirectly proportional to the increase in the number of supports, with the highest observed in specimen with 2 supports, showing increased ductile behaviour with fewer supports as demonstrated in Fig. 16. Nevertheless, all specimens containing fibre exhibited higher impact residual strength ratios, highlighting their capability to retain a significant portion of their original strength after exposure to impact loading. A similar improvement was reported by Lo et al. [49] and Yew et al. [48].

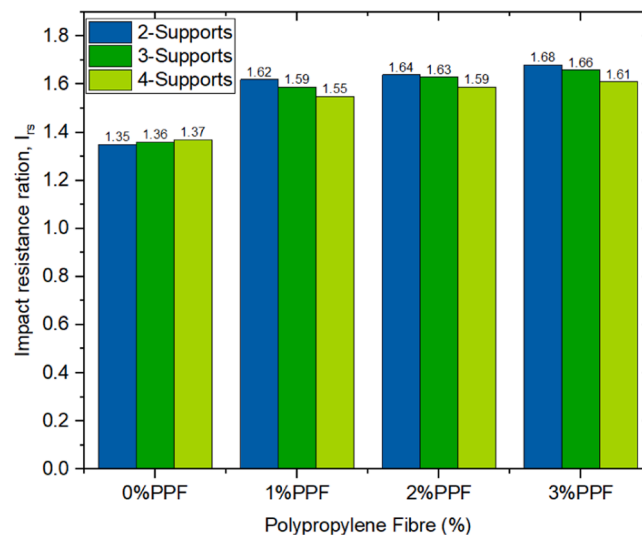


Fig. 19. Impact residual ratio I_{RS} .

5. Conclusions

The study investigated the structural behaviour of lightweight fibre-reinforced Oil Palm shell (OPS) concrete when subjected to low-velocity impact loadings. Considering complete replacement of the natural aggregate with OPS together with PPF within 0–5 %. While the control sample contains only a PPF mesh at the mid-layer, other specimens contain varying volume fractions of PPF at the bottom layer in addition to the mesh. The structural performance of the concrete has been explored in terms of impact energy absorption, crack resistance and residual strength for different boundary conditions and failure modes. The findings highlighted a general improvement in impact and crack resistance with higher boundary conditions and PPF content.

According to the findings presented, the following conclusions are drawn:

1. The overall impact energy absorptions and crack resistance performance of the lightweight-OPS concrete improved with varying PPF and boundary conditions.
2. The inclusion of PPF in boundary conditions does not influence crack length, width, or even the residual strength of the OPS concrete. But significantly control crack propagation.
3. Improved crack resistance results from higher impact energy absorption at the service stage, which sharply declines at the ultimate stage, reaching optimum resistance at 3 % fibre content.
4. Specimens with 8 boundary conditions and 5 % PPF achieved up to 10 and 22 times improvement in impact energy absorption, and up to 25 and 29 times improvement in crack resistance under service and ultimate loading, respectively.
5. A direct correlation between crack resistance and PP fibre and an inverse correlation with boundary conditions was established.
6. Impact residual strength increases in direct proportion to the fibre volume fraction and is inversely proportional to the boundary conditions.

CRediT authorship contribution statement

Idris Ahmed Ja'e: Writing – review & editing, Writing – original draft, Validation, Software, Methodology, Investigation, Formal analysis, Data curation. **zakaria Che Muda:** Writing – original draft, Resources, Project administration, Methodology, Formal analysis, Conceptualization. **agusril Syamsir:** Visualization, Project administration, Data curation. **Chiemela Victor Amaechi:** Writing – original draft, Visualization, Software, Data curation. **Hamad Almujiab:** Writing – original draft, Visualization, Resources, Funding acquisition. **ali E.A Elshekh:** Software, Resources, Funding acquisition, Data curation. **Maaz Osman Bashir:** Software, Resources, Funding acquisition, Data curation. **Abdulrazak H Almaliki:** Software, Resources, Funding acquisition.

Declaration of Competing Interest

The authors declare that they have no known competing financial interests or personal relationships that could have appeared to influence the work reported in this paper.

Acknowledgements

The authors would like to express their gratitude to the Higher Institution Centre of Excellence (HICoE), Ministry of Higher

Education (MOHE), Malaysia under the project code 2024001HICOE as referenced in JPT(BPKI)1000/016/018/34(5). Equal appreciation is also extended to Taif University, Saudi Arabia, for supporting this work through project number TU-DSPP-2024–33.

Appendix

Summary of results

Run	Supt	PPF	E_s	E_u	R_s	R_u
1	2	2	297.444	367.02	455.14	746.8649
2	2	5	493.164	643.113	−148.28	−155.596
3	2	3	362.684	459.051	416.98	704.3281
4	3	3	410.476	833.906	558.33	921.3781
5	4	3	458.268	1208.761	711.46	1147.778
6	4	4	523.508	1447.144	560.02	927.0579
7	4	5	588.748	1685.527	245.6	448.0543
8	5	1	375.58	960.498	640.61	970.0183
9	5	3	506.06	1583.616	876.37	1383.528
10	5	5	636.54	2206.734	460.21	763.9043
11	6	2	488.612	1573.736	991.82	1510.965
12	6	5	684.332	2727.941	686.6	1089.104
13	7	3	601.644	2333.326	1241.53	1883.078
14	7	4	666.884	2791.237	1164.64	1782.508
15	8	5	779.916	3770.355	1174.72	1767.554
16	8	3	649.436	2708.181	1441.78	2146.878

Note: Supt = support, PPF= Polypropylene fibre, E_s = impact energy absorption at service loading, E_u = Impact energy absorption at ultimate loading, R_s =crack resistance at service loading, R_u =crack resistance at ultimate loading.

Data availability

The authors do not have permission to share data.

References

- [1] I.A. Ja'e, et al., Modelling and optimisation of the structural performance of lightweight polypropylene fibre-reinforced LECA concrete, *Results Eng.* 24 (2024) 103149, <https://doi.org/10.1016/j.rineng.2024.103149>.
- [2] M.Z. Al-mulali, H. Awang, H.P.S. Abdul Khalil, Z.S. Aljoumaily, The incorporation of oil palm ash in concrete as a means of recycling: a review, *Cem. Concr. Compos.* 55 (2015) 129–138, <https://doi.org/10.1016/j.cemconcomp.2014.09.007>.
- [3] H.M. Hamada, B. Skariah Thomas, B. Tayeh, F.M. Yahaya, K. Muthusamy, J. Yang, Use of oil palm shell as an aggregate in cement concrete: a review, *Constr. Build. Mater.* 265 (2020) 120357, <https://doi.org/10.1016/j.conbuildmat.2020.120357>.
- [4] J.N. Farahani, P. Shafigh, B. Alsubari, S. Shahnazar, H.B. Mahmud, Engineering properties of lightweight aggregate concrete containing binary and ternary blended cement, *J. Clean. Prod.* 149 (2017) 976–988.
- [5] M. Kareem, A. Raheem, K. Oriola, R. Abdulwahab, A review on application of oil palm shell as aggregate in concrete-Towards realising a pollution-free environment and sustainable concrete, *Environ. Chall.* 8 (2022) 100531.
- [6] M. Aslam, P. Shafigh, M.Z. Jumaat, High strength lightweight aggregate concrete using blended coarse lightweight aggregate origin from palm oil industry, *Sains Malays.* 46 (4) (2017) 667–675.
- [7] Rahman, N.A., Tan, A., Waqbitu, F., and Roslan, N., (Year).The effectiveness of oil palm shell (OPS) as major aggregate replacement in concrete, in IOP Conference Series: Earth and Environmental Science, 2020, vol. 476, no. 1: IOP Publishing, p. 012019.
- [8] M. Mannan, J. Alexander, C. Ganapathy, D. Teo, Quality improvement of oil palm shell (OPS) as coarse aggregate in lightweight concrete, *Build. Environ.* 41 (9) (2006) 1239–1242.
- [9] K.H. Mo, S.P. Yap, U.J. Alengaram, M.Z. Jumaat, C.H. Bu, Impact resistance of hybrid fibre-reinforced oil palm shell concrete, *Constr. Build. Mater.* 50 (2014) 499–507.
- [10] M. Maghfouri, P. Shafigh, M. Aslam, Optimum oil palm shell content as coarse aggregate in concrete based on mechanical and durability properties, *Adv. Mater. Sci. Eng.* 2018 (2018) 1–14.
- [11] S.P. Yap, C.H. Bu, U.J. Alengaram, K.H. Mo, M.Z. Jumaat, Flexural toughness characteristics of steel–polypropylene hybrid fibre-reinforced oil palm shell concrete, *Mater. Des.* 57 (2014) 652–659.
- [12] M. Nili, A. Ghorbankhani, A. AlaviNia, M. Zolfaghari, Assessing the impact strength of steel fibre-reinforced concrete under quasi-static and high velocity dynamic impacts, *Constr. Build. Mater.* 107 (2016) 264–271.
- [13] C.V. Amaechi, A. Reda, I.A. Ja'e, C. Wang, C. An, Guidelines on composite flexible risers: monitoring techniques and design approaches, *Energies* 15 (14) (2022) 4982.
- [14] C. Wang, J. Yuan, B. Lu, Y. Zhang, Z. Ma, New insights into the mechanical behavior and enhancement mechanism of micro-steel-fiber-reinforced recycled aggregate concrete through in-situ 4D CT analysis, *Constr. Build. Mater.* 438 (2024) 137111, <https://doi.org/10.1016/j.conbuildmat.2024.137111>.
- [15] C. Wang, Z. Du, Y. Zhang, Z. Ma, Elaborating the 3D microstructural characteristics and strength softening mechanical mechanism of fiber-reinforced recycled aggregate concrete, *Constr. Build. Mater.* 436 (2024) 137009, <https://doi.org/10.1016/j.conbuildmat.2024.137009>.
- [16] C. Wang, J. Guo, L. Cao, Y. Zhang, C. Li, Z. Ma, Mechanical behavior and fiber reinforcing mechanism of high-toughness recycled aggregate concrete under high strain-rate impact loads, *Constr. Build. Mater.* 437 (2024) 136960, <https://doi.org/10.1016/j.conbuildmat.2024.136960>.

- [17] C. Wang, Z. Du, Microscopic interface deterioration mechanism and damage behavior of high-toughness recycled aggregate concrete based on 4D in-situ CT experiments, *Cem. Concr. Compos.* 153 (2024) 105720, <https://doi.org/10.1016/j.cemconcomp.2024.105720>.
- [18] C.-L. Hwang, V.-A. Tran, J.-W. Hong, Y.-C. Hsieh, Effects of short coconut fiber on the mechanical properties, plastic cracking behavior, and impact resistance of cementitious composites, *Constr. Build. Mater.* 127 (2016) 984–992.
- [19] M. Saidani, D. Saraireh, M. Gerges, Behaviour of different types of fibre reinforced concrete without admixture, *Eng. Struct.* 113 (2016) 328–334.
- [20] M. Mastali, A. Dalvand, The impact resistance and mechanical properties of self-compacting concrete reinforced with recycled CFRP pieces, *Compos. Part B: Eng.* 92 (2016) 360–376.
- [21] H. Cifuentes, F. García, O. Maeso, F. Medina, Influence of the properties of polypropylene fibres on the fracture behaviour of low-, normal-and high-strength FRC, *Constr. Build. Mater.* 45 (2013) 130–137.
- [22] A.A.E. Aliabdo, A.E.M. Abd Elmoaty, M. Hamdy, Effect of internal short fibers, steel reinforcement, and surface layer on impact and penetration resistance of concrete, *Alex. Eng. J.* 52 (3) (2013) 407–417.
- [23] R. Bagherzadeh, H.R. Pakravan, A.-H. Sadeghi, M. Latifi, A.A. Merati, An investigation on adding polypropylene fibers to reinforce lightweight cement composites (LWC), *J. Eng. Fibers Fabr.* 7 (4) (2012), 155892501200700410.
- [24] C.V. Amaechi, et al., Numerical study on plastic strain distributions and mechanical behaviour of a tube under bending, *Inventions* 7 (1) (2022) 9.
- [25] J. Yahaghi, Z.C. Muda, S.B. Beddu, Impact resistance of oil palm shells concrete reinforced with polypropylene fibre, *Constr. Build. Mater.* 123 (2016) 394–403.
- [26] I.A. Ja'e, M.O.A. Ali, A. Yenduri, Z. Nizamani, A. Nakayama, Effect of various mooring materials on hydrodynamic responses of turret-moored FPSO with emphasis on intact and damaged conditions, *J. Mar. Sci. Eng.* 10 (4) (2022) 453.
- [27] M.K. Yew, H.B. Mahmud, B.C. Ang, M.C. Yew, Influence of different types of polypropylene fibre on the mechanical properties of high-strength oil palm shell lightweight concrete, *Constr. Build. Mater.* 90 (2015) 36–43.
- [28] A. Islam, U.J. Alengaram, M.Z. Jumaat, N.B. Ghazali, S. Yusoff, I.I. Bashar, Influence of steel fibers on the mechanical properties and impact resistance of lightweight geopolymer concrete, *Constr. Build. Mater.* 152 (2017) 964–977.
- [29] Zamzani, N.M., Mydin, A.O., and Ghani, A.N.A., (Year). Experimental investigation on engineering properties of lightweight foamed concrete (LFC) with coconut fiber addition, in *MATEC Web of Conferences*, 2018, vol. 250: EDP Sciences, p. 05005.
- [30] S. Kanchidurai, E. Madhumithra, P. Jaishankar, R. Shivani, M. Rithani, Experimental Investigation on Hybrid Fibre-reinforced Concrete (HFRCC) fracture toughness and impact resistance with partial replacement of nano-silica, *Mater. Today: Proc.* (2023).
- [31] Y.-F. Li, K.-F. Lee, G.K. Ramanathan, T.-W. Cheng, C.-H. Huang, Y.-K. Tsai, Static and dynamic performances of chopped carbon-fiber-reinforced mortar and concrete incorporated with disparate lengths, *Materials* 14 (4) (2021) 972.
- [32] J.E. IA, T. Sulaiman, A. Abdurrahman, Evaluation of pozzolanic materials and their influence on cement and workability retention of concrete, *Niger. J. Sci. Res.* 18 (4) (2019) 329–336.
- [33] Ö. Anil, E. Kantar, M.C. Yilmaz, Low velocity impact behavior of RC slabs with different support types, *Constr. Build. Mater.* 93 (2015) 1078–1088.
- [34] C. Kankam, Impact resistance of palm kernel fiber-reinforced concrete pavement slab, *J. Ferrocem.* 29 (4) (1999) 279–286.
- [35] G. Ramakrishna, T. Sundararajan, Impact strength of a few natural fibre reinforced cement mortar slabs: a comparative study, *Cem. Concr. Compos.* 27 (5) (2005) 547–553.
- [36] A.T. Nair, A.R. Makwana, M.M. Ahammed, The use of response surface methodology for modelling and analysis of water and wastewater treatment processes: a review, *Water Sci. Technol.* 69 (3) (2014) 464–478.
- [37] M.A. Hadiyat, B.M. Sopha, B.S. Wibowo, Response surface methodology using observational data: a systematic literature review, *Appl. Sci.* 12 (20) (2022) 10663.
- [38] A. Zaki, S. Yadi, E. Khoirullianum, R. Suganda, C.A. Wibisono, Effect of partial replacement of aggregate with oil palm shell on compressive and flexural strength of fiber concrete, *Multidiscip. Sci. J.* 6 (7) (2024) 2024102. -2024102.
- [39] M.H.R. Sobuz, et al., Mechanical properties and flexural response of palm shell aggregate lightweight reinforced concrete beam, *Sustainability* 15 (22) (2023) 15783.
- [40] Muda, Z.C. et al., (Year). Impact resistance performance of green construction material using light weight oil palm shells reinforced bamboo concrete slab, in *IOP Conference Series: Earth and Environmental Science*, 2013, vol. 16, no. 1: IOP Publishing, p. 012063.
- [41] K.H. Mo, P. Visintin, U.J. Alengaram, M.Z. Jumaat, Prediction of the structural behaviour of oil palm shell lightweight concrete beams, *Constr. Build. Mater.* 102 (2016) 722–732.
- [42] R.Z. Al-Rousan, M.A. Alhassan, H. Al-Salman, Impact resistance of polypropylene fiber reinforced concrete two-way slabs, *Struct. Eng. Mech.* 62 (3) (2017) 373–380.
- [43] A.A.A. Samad, J. Hadipramana, A.Z. Ahmad Mujahid, N. Mohamad, Investigation on energy absorption of slab foamed concrete reinforced by polypropylene fibre subjected to impact loading, *Adv. Mater. Res.* 831 (2014) 67–72.
- [44] I.A. Ja'e, et al., Optimisation of mechanical properties and impact resistance of basalt fibre reinforced concrete containing silica fume: Experimental and response surface assessment, *Dev. Built Environ.* 17 (2024) 100368, <https://doi.org/10.1016/j.dibe.2024.100368>.
- [45] P. Song, S. Hwang, B. Sheu, Strength properties of nylon-and polypropylene-fiber-reinforced concretes, *Cem. Concr. Res.* 35 (8) (2005) 1546–1550.
- [46] S. Kakooei, H.M. Akil, M. Jamshidi, J. Rouhi, The effects of polypropylene fibers on the properties of reinforced concrete structures, *Constr. Build. Mater.* 27 (1) (2012) 73–77.
- [47] C.-G. Han, Y.-S. Hwang, S.-H. Yang, N. Gowripalan, Performance of spalling resistance of high performance concrete with polypropylene fiber contents and lateral confinement, *Cem. Concr. Res.* 35 (9) (2005) 1747–1753.
- [48] M.K. Yew, M.C. Yew, B.C. Ang, J.H. Beh, F.W. Lee, Strength properties and toughness indices of hybrid polymeric fibre reinforced renewable oil palm shell concrete, *Key Eng. Mater.* 929 (2022) 143–148.
- [49] L.T. Loh, et al., Mechanical and thermal properties of synthetic polypropylene fiber-reinforced renewable oil palm shell lightweight concrete, *Materials* 14 (9) (2021) 2337.